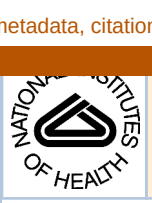

Published in final edited form as:
Mol Cell. 2010 February 12; 37(3): 408–417. doi:10.1016/j.molcel.2009.12.038.

Unconventional Ubiquitin Recognition by the Ubiquitin-Binding Motif within the Y-Family DNA Polymerases ι and Rev1

Martha G. Bomar[1,4], **Sanjay D'Souza**[2,4], **Marzena Bienko**[3], **Ivan Dikic**[3], **Graham C. Walker**[2], and **Pei Zhou**[1,*]

[1] Department of Biochemistry, Duke University Medical Center, Durham, NC 27710, USA

[2] Department of Biology, Massachusetts Institute of Technology, Cambridge, MA 02139, USA

[3] Institute of Biochemistry II and Cluster of Excellence Macromolecular Complexes, Goethe University, Frankfurt, Germany

SUMMARY

Translesion synthesis is an essential cell survival strategy to promote replication after DNA damage. The accumulation of the Y-family polymerases (pol) ι and Rev1 at the stalled replication machinery is mediated by the ubiquitin-binding motifs (UBMs) of the polymerases and enhanced by PCNA monoubiquitination. We report the solution structures of the C-terminal UBM of human pol ι and its complex with ubiquitin. Distinct from other ubiquitin-binding domains, the UBM binds to the hydrophobic surface of ubiquitin centered at L8. Accordingly, mutation of L8A, but not I44A of ubiquitin abolishes UBM binding. Human pol ι contains two functional UBMs, both of which contribute to replication foci formation. In contrast, only the second UBM of *Saccharomyces cerevisiae* Rev1 binds to ubiquitin and is essential for Rev1-dependent cell survival and mutagenesis. Point mutations disrupting the UBM-ubiquitin interaction also impair the accumulation of pol ι in replication foci and Rev1-mediated DNA damage tolerance *in vivo*.

Keywords

polymeraseι; Rev1; translesion synthesis; UBM; ubiquitin-binding domain

INTRODUCTION

DNA lesions caused by endogenous and exogenous damaging agents block the activity of high-fidelity replicases at the replication fork and hinder the faithful duplication of genomic information. In addition to employing highly complex repair mechanisms, cells utilize specialized DNA polymerases to synthesize DNA across the lesion sites (translesion synthesis, TLS) to promote cell survival and genomic integrity. The majority of the polymerases involved in translesion synthesis belong to the Y-family of DNA polymerases that are characterized by

*Correspondence: peizhou@biochem.duke.edu.
[4]These authors contributed equally to this work

Accession Numbers
The coordinates of the human pol ι UBM2 and its complex with ubiquitin have been deposited in the Protein Data Bank with the accession codes **2KHU** and **2KHW**, respectively.

a less stringent active site and lower processivity compared to the high-fidelity replicases (Ohmori et al., 2001). Although these TLS polymerases are able to accommodate a variety of DNA lesions, including large bulky adducts, they are frequently mutagenic when replicating undamaged DNA. Therefore, the switch between the TLS polymerases and high-fidelity replicases at the stalled replication fork during active DNA replication is tightly regulated.

Recent studies suggest that the accumulation of the TLS polymerases at the stalled replication fork is mediated by the monoubiquitination of the proliferating cell nuclear antigen (PCNA) in response to DNA damage (Hoege et al., 2002; Kannouche et al., 2004). This activity also depends on the presence of the highly conserved ubiquitin-binding domains within the polymerases: notably, the ubiquitin-binding motif (UBM) of pol ι and Rev1 and the ubiquitin-binding zinc finger (UBZ) of pol η and pol κ (Bienko et al., 2005; Plosky et al., 2006). Monoubiquitination of PCNA enhances the basal interaction between PCNA and the Y-family polymerases and increases the residence time of the TLS polymerases in the replication foci (Bienko et al., 2005; Guo et al., 2008; Kannouche et al., 2004; Sabbioneda et al., 2008; Watanabe et al., 2004). The specific requirement of the ubiquitin-binding domains of the TLS polymerases for cell survival after DNA damage and for damage-induced enhancement of the residence time of the TLS polymerases in the replication foci *in vivo* suggests that the interactions between the UBM and UBZ domains of Y-family polymerases and monoubiquitinated PCNA are essential for translesion synthesis.

We previously reported the solution structure of the UBZ domain of human pol η as a classical C_2H_2 zinc finger with a ββα fold. The UBZ domain binds to the canonical hydrophobic surface of ubiquitin, defined by L8, I44, H68, and V70 (Bomar et al., 2007). In contrast to the UBZ domain and the vast majority of known ubiquitin-binding domains, the UBM was characterized by its unique ability to interact with an I44A ubiquitin mutant (Bienko et al., 2005).

Two UBMs separated by ~30–190 amino acids are found within the C-terminal part of pol ι and Rev 1. Although both of these UBMs in pol ι bind to ubiquitin and are required for accumulation of pol ι in the replication foci, we show that only the second UBM of *Saccharomyces cerevisiae* Rev1 (yeast Rev1) is a bona fide ubiquitin receptor and is required for cell survival and mutagenesis. To understand the molecular basis underlying the $I44_{Ub}$-independent UBM-ubiquitin interaction and its role in translesion synthesis, we determined the solution structures of the C-terminal UBM (UBM2) of human pol ι and its complex with ubiquitin. The binding between UBM2 and ubiquitin was probed by NMR and isothermal titration calorimetry (ITC). We show that point mutants that diminish UBM-ubiquitin binding also result in reduced localization to replication foci for pol ι. Likewise, alanine substitution of the corresponding ubiquitin-interacting residues in yeast Rev1 impairs Rev1 function *in vivo*.

RESULTS

Not all UBMs Are Engaged in Ubiquitin Binding

Both pol ι and Rev1 contain two highly conserved UBMs in the C-terminal part of the protein. To evaluate the ubiquitin-binding properties of these UBMs, we individually purified the UBMs from human pol ι and yeast Rev1 as GB1-fusion proteins for increased solubility and stability (Zhou et al., 2001) and monitored their interaction with ubiquitin using NMR titration. Addition of unlabeled human ubiquitin to ^{15}N-labeled human pol ι UBM1 or UBM2 resulted in progressive perturbation for a subset of the UBM resonances (data not shown), indicating that both UBM1 and UBM2 of pol ι are functional ubiquitin-binding domains. Interestingly, titration of ^{15}N-labeled *S. cerevisiae* Rev1 UBMs with unlabeled yeast ubiquitin only perturbed the resonances of UBM2, but not UBM1 (Figure S1), suggesting that UBM2 but not UBM1 is the functional ubiquitin-binding domain in *S. cerevisiae* Rev1. This *in vitro* observation is

consistent with previous results showing that mutation of the highly conserved "Leu-Pro" motif in the *S. cerevisiae* Rev1 UBM1 does not affect its function *in vivo*, whereas mutation of the same motif in UBM2 has profound defects on the survival and mutagenesis of cells following DNA damage (D'Souza et al., 2008; Guo et al., 2006b).

Solution Structure of the Human Pol ι UBM2

Due to the essential role of the UBMs of pol ι and Rev1 in response to DNA damage and translesion synthesis, we determined the solution structure of the human pol ι UBM2 (Figure 1). Except for residues at the termini, the UBM domain is well structured, with mean pairwise RMSD values of 0.33 Å and 1.17 Å for the backbone and heavy atoms of residues 676–707, respectively. Additional statistics on the structural ensemble are given in Supplementary Table S1.

Using analytical ultracentrifugation, we found that the UBM2 exists as a monomer in solution (data not shown). The structure of UBM2 consists of two amphipathic helices that are supported by an N-terminal loop extending across the C-terminal helix at a perpendicular angle. The N-terminal loop adopts a typical β-strand conformation, with the side chains of two hydrophobic residues (I677 and F679) juxtaposed to interact with the hydrophobic surfaces of the two helices (α1 and α2) following it. Helix 1 contains a single turn (P685 to F688) and is positioned at a sharp angle with respect to the N-terminal loop. The stability of this short helix is greatly enhanced by the presence of two prototypical N-terminal helix cap residues (Richardson and Richardson, 1988), D684 and P685, with the side chain of D684 forming hydrogen bonds with the amides of Q686 and V687. The C-terminal helix (α2) is significantly longer than helix 1, extending from residue E693 to R705. The two helices lie within a plane at an angle of ~50–60 degrees and are connected by a short loop containing the signature "Leu-Pro" motif that is poised for interaction with ubiquitin. The two helices and the N-terminal loop are packed together by a core of aromatic residues, including F679 of the loop, F688 of α1, and W703 of α2 (Figure 1B); the stability of this aromatic core is further supported by surrounding hydrophobic residues including I677 of the loop, I683, Y689 and L691 flanking helix 1, and V695, L699 and L700 of helix 2 (Figure 1C).

Although many of the hydrophobic residues observed in human pol ι UBM2 are highly conserved among all UBMs, W703 of helix 2 is frequently replaced by a Lys residue in UBM1 (Figure 1C), suggesting that helix 2 of these UBMs may be substantially shorter than that of pol ι UBM2. Notably, an analysis of the UBM2 structure with the DALI server did not identify any known structure with a similar fold.

Ubiquitin Recognition by the UBM2 of Human Pol ι

To understand the molecular basis for the I44-independent ubiquitin recognition by the UBM, we further determined the solution structure of the human pol ι UBM2-ubiquitin complex by NMR (Figure 2; see Supplementary Table S2 for structural statistics). The overall structures of UBM2 and ubiquitin in the UBM2-ubiquitin complex are similar to those of the free proteins, with average ensemble backbone RMSD values of 0.45 Å and 0.53 Å for UBM2 and ubiquitin, respectively, suggesting that neither ubiquitin nor UBM2 displays a significant conformational change upon complex formation.

The ubiquitin moiety adopts an α/β-roll topology with an α-helix and a 3_{10}-helix packing against a β-sheet containing five strands. A hydrophobic surface, located on the solvent-exposed surface of the β-sheet and known for interacting with most ubiquitin-binding domains, is recognized by residues from the two helices of UBM2; however, the overall binding area is noticeably shifted toward L8 instead of centering at I44 (Figure 2), a critical residue for most ubiquitin-binding domain (UBD)-ubiquitin interactions (Chen and Sun, 2009).

A set of hydrophobic residues of UBM2, including I683 located to the N-terminal of helix 1, V687 and F688 of helix 1, L691 and P692 of the invariant "Leu-Pro" motif connecting helices α1 and α2, and V695, L699, and W703 of α2, form a network of hydrophobic interactions encircling L8 and V70 of ubiquitin. This core binding interface is flanked by peripheral hydrophobic interactions formed between V687, L691, P692 and V695 of UBM2 and I44 and the aliphatic side chains of K6 and H68 of ubiquitin. The previously discovered "Leu^{691}-Pro^{692}" motif of UBM2 plays an important role in supporting ubiquitin binding, with the side chains of L691 inserting into the hydrophobic pocket of ubiquitin defined by L8, I44, H68 and V70, and P692 nudging into the shallow surface groove formed by I44, G47 and Q49. Our ITC measurements showed that alanine substitution of either L691 or P692 significantly reduced the UBM2-ubiquitin binding, and the L691A/P692A double mutation abolished the interaction (Table 1). Interestingly, the ^{1}H-^{15}N HSQC spectrum of the L691A/P692A UBM2 double mutant revealed extensive resonance perturbation for many residues distant to the mutated Leu^{691}-Pro^{692} motif (data not shown), suggesting that the loss of ubiquitin-binding affinity of this double mutant likely reflected a disruption of the UBM2 structure in addition to an interference of the ubiquitin-binding interface.

Consistent with the structurally observed L8-centric mode of interaction, mutation of $L8A_{Ub}$ completely abolished the UBM2-ubiquitin interaction; mutation of $V70A_{Ub}$ reduced the binding affinity of wild-type ubiquitin from 15 μM to 167 μM, whereas the I44A or H68A ubiquitin mutants had the least effect on the UBM2-binding affinity (83 or 62 μM, respectively). Likewise, alanine substitution of the complementary hydrophobic residues in UBM2, including I683, V687, F688, V695 and L699, all reduced the UBM2-ubiquitin binding affinity (Table 1).

The interaction between ubiquitin and UBM2 also appears to depend critically on the stability of the N-terminal short helix in UBM2. Alanine substitution of D684, the N-cap residue of helix 1 in UBM2, disrupted the UBM2-ubiquitin binding. In addition to the structural role of D684 as a helix cap, its amide group forms a hydrogen bond with the carbonyl group of L8 of ubiquitin, thus providing an anchoring point for ubiquitin binding. Supporting this observation, numerous intermolecular NOEs are observed between the amide group of D684 of UBM2 and Hα and Hβ of L8, Hα and Hβ of T9, and Hα protons of G10 of ubiquitin. Additionally, the side chain of E690, a residue immediately before the "Leu-Pro" motif, forms a hydrogen bond with the side chain of H68 and is well positioned to form a salt bridge with K6 of ubiquitin.

A subset of the UBM2-ubiquitin intermolecular NOEs is depicted in Figure 2E.

Structural Basis of the Ubiquitin-Binding Specificity of *S. cerevisiae* Rev1 UBMs

The solution structure of the pol ι UBM2-ubiquitin complex provides a molecular framework to explain why *S. cerevisiae* Rev1 UBM1 does not bind ubiquitin, whereas its UBM2 does. A sequence alignment of the UBMs among various species of Rev1 and pol ι shows that the yeast Rev1 UBM1 contains nearly all of the highly conserved residues, including the invariant "Leu-Pro" motif and numerous residues along the ubiquitin-binding interface (Figure 1C). However, two functionally important residues are noticeably different in the yeast Rev1 UBM1. The first residue is D684 in UBM2 of pol ι, which is replaced by T756 in *S. cerevisiae* Rev1 UBM1. This highly conserved Asp residue (occasionally replaced by Glu) serves as an N-cap to stabilize the short helix (α1) in the UBM, and its substitution by Ala disrupted UBM2-ubiquitin binding (Table 1). Although Thr is also a good helix cap, as its hydroxyl group can form a hydrogen bond to the helix, its side chain methyl group is positioned to generate van der Waals clashes with the β1-β2 loop of ubiquitin, thus interfering with ubiquitin binding. Indeed, the binding affinity of the D684T mutant of the human pol ι UBM2 (>400 μM) was significantly reduced from the wild-type protein (15 μM; Table 1). Similarly, replacing the highly conserved V687, which interacts with L8 of ubiquitin, with an Ala residue (A759) in *S. cerevisiae* Rev1

UBM1 is expected to impair ubiquitin binding. Indeed, the V687A pol ι UBM2 mutant displayed a reduced binding affinity toward ubiquitin (94 μM; Table 1).

Disruption of UBM-Ubiquitin Binding Impairs Pol ι Foci Accumulation

Pol ι contains two functional UBMs, and deletion of both UBMs abolishes the ability of pol ι to form replication foci after UV damage (Bienko et al., 2005). Observations of asynchronized cells revealed that both pol ι and pol η constitutively localize to replication forks during unperturbed S phase, and their accumulation in foci requires functional ubiquitin-binding domains (Guo et al., 2006b). Recently, Sabbioneda and co-workers showed that pol η is transiently immobilized in the replication foci and that monoubiquitination of PCNA enhances but is not required for its foci formation (Sabbioneda et al., 2008). Taken together, these studies suggest that the ubiquitin-binding domains of Y-family polymerases serve a dual function: recruiting polymerases to replication foci and facilitating their interaction with PCNA under DNA damage conditions.

To evaluate the functional role of the UBMs and establish the connection between the ubiquitin-binding property of individual UBMs and polι's ability to localize to replication foci, we compared mouse pol ι constructs containing either the UBM1 or UBM2 deletion with the wild-type protein for their ability to accumulate in replication foci during S phase (Figure 3A). For cells transfected with the wild-type EYFP-pol ι construct, replication foci were observed in 22.9 ± 2.3% of cells, which corresponds to the average percentage of cells in S phase. No replication foci accumulation was observed for cells transfected with pol ι constructs with either a UBM1 or UBM2 deletion, suggesting that both of these UBMs are required for the proper recruitment of pol ι to the replication foci.

In parallel, we examined the effect on foci formation for single point mutations in human pol ι UBM2 that negatively affect ubiquitin binding (Figure 3B and C). For the D684A mutant, only 11.9 ± 1.3% of the transfected cells showed foci formation, whereas the percentage was even smaller for the V687A mutant (8.0 ± 0.5%). The most dramatic effect was observed for the F688A mutant, which essentially eliminated foci formation (0.2 ± 0.3%). To evaluate if these point mutations also affected the UBM2 structure, we recorded the ^{1}H-^{15}N HSQC spectra of the D684A, V687A, and F688A mutants. Both the D684A and V687A UBM2 mutants displayed ^{1}H-^{15}N HSQC spectra similar to that of the wild-type protein, whereas there were large changes within the ^{1}H-^{15}N HSQC spectrum of the F688A UBM2 mutant (data not shown). These observations suggest that neither the D684A nor V687A mutation affected the structural integrity of the UBM2. Thus, the impaired abilities of these two mutants to accumulate at the replication foci exclusively reflect their reduced ubiquitin-binding affinities. In contrast, the alanine substitution of F688, which is an essential residue both for the ubiquitin binding and the proper folding of UBM2, disrupted the global fold of the UBM2 and completely abolished foci formation similarly to the pol ι UBM2 deletion mutant. The direct correlation of the ubiquitin-binding affinities of diverse pol ι UBM2 point mutants with their ability to localize to replication foci highlights the functional significance of the UBM2-ubiquitin interaction.

Role of Rev1 UBM2-Ubiquitin Interaction in Response to DNA Damage

In light of the central role of Rev1 in the process of mutagenic replicative bypass of damaged DNA, we examined whether the *S. cerevisiae* Rev1 UBM2 residues corresponding to the ubiquitin-interacting residues of human pol ι UBM2 are required for Rev1-mediated cell survival and mutagenesis. Wild-type or mutant *REV1* alleles under the native Rev1 promoter were used to complement the DNA damage sensitivity defect of the *rev1Δ* strain. Strikingly, point mutation of F817A, L821A, I825A and V829A or double mutation of E814A/M818A (corresponding to human pol ι UBM2 residues V687, L691, V695, L699, and D684/F688,

respectively; Figure 1C) largely inactivated Rev1 function in cell survival after methyl methanesulfonate (MMS) treatment as well as after UV irradiation (Figure 4A). The most dramatic effect was seen for the alanine substitution of L821 (equivalent to pol ι L691) from the "Leu-Pro" signature motif. In contrast, mutation of M813A had little effect on the ability of Rev1 to complement the DNA damage sensitivity of the *rev1Δ* strain. Consistent with this observation, the corresponding human pol ι UBM2 mutant I683A had the least effect on the UBM2-ubiquitin affinity (Table 1).

To determine if these UBM2 mutations also impair Rev1 function in mutagenesis, we examined *S. cerevisiae* strains harboring a subset of the Rev1 UBM2 mutants for their ability to revert the *ade2-1* allele after a low dose of UV irradiation. We found that the survival-deficient UBM2 mutants E814A/M818A, F817A, L821A and V829A in Rev1 also showed reduced rates of UV-induced mutagenesis, whereas the M813A mutation had no effect on the mutation frequency when compared to cells expressing wild-type Rev1 (Figure 4B). Taken together, these results indicate that an effective UBM2-ubiquitin interaction is required for *S. cerevisiae* Rev1 function *in vivo*.

DISCUSSION

Distinct Ubiquitin Recognition by UBM

In addition to possessing a previously unobserved protein fold, the UBM also binds ubiquitin in a manner distinct from all known ubiquitin-binding domains. Among the protein domains that recognize monoubiquitin through helical interactions, the UIM, MIU/IUIM and UBZ all employ a single helix to bind the solvent-exposed β-sheet of ubiquitin (Bomar et al., 2007; Hirano et al., 2006; Lee et al., 2006; Penengo et al., 2006; Swanson et al., 2003; Wang et al., 2005), with the ubiquitin-binding helix oriented either parallel or anti-parallel to the central β-strand of ubiquitin. In contrast, the UBM binds ubiquitin primarily through two consecutive helices, with helix 1 oriented almost perpendicular to the central β-strand of ubiquitin and with helix 2 poised at an angle (Figure 5A). Although other ubiquitin-binding domains, such as the UBA and CUE domains (Chang et al., 2006; Kang et al., 2003; Ohno et al., 2005; Swanson et al., 2006), also bind ubiquitin through two helices, these ubiquitin-binding helices are discontinuous, coming from the first and third helices of the three-helix bundle, and are arranged in an "up-up" topology, whereas the UBM utilizes two consecutive helices arranged in an "up-down" topology for ubiquitin binding (Figure 5B). The GAT domain, another ubiquitin-binding domain with a three-helix bundle architecture, also binds ubiquitin through its first and second helices (Figure 5C) (Akutsu et al., 2005; Prag et al., 2005). However, these two ubiquitin-interacting helices are longer and closer to being parallel. In comparison, the UBM helices are noticeably shorter and are positioned within a plane at a large angle of ~50–60 degrees to each other; these helices, together with the α1-α2 loop containing the signature "Leu-Pro" motif, define an expanded interaction surface for ubiquitin recognition centered at L8 instead of I44.

Role of UBM-Ubiquitin Interaction in DNA Damage Response

Human and mouse pol ι and REV1 each contain two copies of functional UBMs (Bienko et al., 2005; Guo et al., 2006b). Although *S. cerevisiae* Rev1 also contains two UBMs, only the UBM2 is a bona fide ubiquitin-binding domain and is required for Rev1 function in yeast (D'Souza et al., 2008; Guo et al., 2006b; Wood et al., 2007). Our study provides the first structural interpretation of the binding specificity of the two UBMs in *S. cerevisiae* Rev1 and their functional discrepancy. Given that one functional UBM is sufficient for the activity of *S. cerevisiae* Rev1 *in vivo*, it is intriguing to speculate why both of the UBMs of mammalian pol ι and REV1 are required for proper function.

In mouse REV1, deletion of either the UBM1 or UBM2 diminishes damage-induced foci formation, whereas deletion of both UBMs abolishes this UV-induced effect (Guo et al., 2006b). Neither of these UBM mutants affects foci formation at the basal level (i.e., without UV damage), which is mediated by the PCNA-interacting BRCT domain (Guo et al., 2006a; Guo et al., 2006b). These observations suggest that the UBMs and the BRCT domain in REV1 have separate functions, with the BRCT domain constitutively recruiting REV1 to replication foci, and the UBMs directing REV1 to arrested replication forks in cells that have sustained DNA damage, most likely through a single UBM interaction with monoubiquitinated PCNA. In this case, a second UBM is free to engage another ubiquitinated replication factor in translesion synthesis.

The UBMs appear to have a more prominent effect on pol ι function. Our results show that the foci accumulation of pol ι in the S phase of undamaged cells requires two functional UBMs. Deletion of either of the two UBMs of pol ι abolishes its accumulation at the replication foci. Furthermore, point mutation of a single UBM (such as UBM2) that diminishes ubiquitin binding is sufficient to impair pol ι activity *in vivo*. Because there is minimal monoubiquitination of PCNA in undamaged cells, these observations suggest that the UBMs of pol ι are engaged in the recognition of other translesion factors, most likely in the ubiquitinated form, in the replication foci.

In this regard, it is worth noting that besides PCNA, translesion polymerases or subunits of the polymerase δ can also be ubiquitinated (Bienko et al., 2005; Guo et al., 2006b; Liu and Warbrick, 2006). Therefore, the UBMs may serve a scaffolding function to recruit ubiquitinated replication factors for the synergistic assembly of the multi-component translesion synthesis machinery, a process that can be further enhanced by monoubiquitination of PCNA. The absolute requirement of functional UBMs for pol ι and Rev1 activity *in vivo* suggests that the UBM-mediated interaction network plays an essential role in translesion synthesis.

A recent bioinformatics study revealed the presence of a UBM in XPG, an endonuclease involved in nucleotide excision repair (Hofmann, 2009). This intriguing discovery indicates a potential role for the UBM to function outside the regulation of the Y-family polymerases, suggesting that the UBM-ubiquitin interaction may be a more general regulatory module in other DNA repair and cellular pathways.

Modulating UBM-Ubiquitin Interaction for Cancer Therapy

Although the biochemical properties of pol ι and Rev1 have been studied in detail, *in vivo* functions of these enzymes are only now being unveiled. For example, pol ι has recently been implicated in UV-induced mutagenesis in Burkitt's lymphoma (Gueranger et al., 2008). Likewise, genes implicated in the chromosome instability syndrome Fanconi anemia have been shown to regulate Rev1 activity (Mirchandani et al., 2008; Niedzwiedz et al., 2004). The recent discovery that inhibition of REV1 greatly reduced the number of carcinogen-induced lung tumors in mice highlights the role of translesion synthesis in cancer development and the therapeutic potential associated with it (Dumstorf et al., 2009). Moreover, in human ovarian carcinoma cells, alteration of the levels of REV1 modulates the cytotoxicity and mutagenesis of the chemotherapeutic drug cisplatin, pointing to a connection between REV1 and the development of chemoresistance *in vivo* (Lin et al., 2006; Okuda et al., 2005). Given the unique structural fold and the distinct ubiquitin-binding mode of the UBM and its essential role for maintaining pol ι and Rev1 function *in vivo*, targeting the UBM-mediated assembly of the damage-tolerance replication machinery may provide an effective approach for cancer treatment or prevention.

EXPERIMENTAL PROCEDURES

Molecular Cloning

The DNA sequences corresponding to the UBM1 or UBM2 of human DNA polymerase ι (residues 491–530 for UBM1 or 674–715 for UBM2) or *S. cerevisiae* Rev1 (residues 747–786 for UBM1 or 804–857 for UBM2) were synthesized; the PCR-amplified DNA was digested and ligated into a modified pET30 vector (EMD Biosciences, Inc.) between the BamHI and XhoI restriction sites to produce an N-terminal GB1- and C-terminal His_6-fused UBM domain construct. The DNA sequences of human or yeast ubiquitin were cloned into the pET15b vector (EMD Biosciences, Inc.). Point mutants of the pol ι and Rev1 UBMs and ubiquitin were prepared using the QuikChange site-directed mutagenesis kit (Stratagene). The presence of the correct inserts of these constructs was confirmed by DNA sequencing. A low-copy pRS416-*REV1* plasmid was used for the yeast assays (D'Souza et al., 2008).

Protein Purification

The GB1-fused UBM constructs were overexpressed in *Escherichia coli* BL21(DE3) STAR cells (Invitrogen) (Zhou et al., 2001). Bacterial cells were induced with 0.25 or 0.5 mM IPTG at 20 °C for 18 hours. The overexpressed proteins were initially purified by a Ni^{2+}-NTA column, followed by size-exclusion chromatography (Superdex 75, GE Healthcare). For the Rev1 UBM purification, the C-terminal His_6 tag was cleaved from the rest of the protein by digestion with Precision protease. N-terminal His_6-tagged human and yeast ubiquitin were overexpressed in and purified from bacterial cells. The His_6-tag of ubiquitin was removed by thrombin cleavage. For NMR studies, isotopically enriched proteins were overexpressed in M9 minimal media using ^{15}N-NH_4Cl and ^{13}C-glucose as the sole nitrogen and carbon sources (Cambridge Isotope Laboratories). All NMR samples were exchanged into a buffer containing 25 mM sodium phosphate, 100 mM KCl, and 10% D_2O or 100% D_2O (pH=7.0) before experiments. UBM and ubiquitin point mutants were overexpressed and purified similarly to the wild-type proteins.

NMR

NMR experiments were conducted at 25 °C using Varian INOVA 600 or 800 MHz spectrometers. Backbone resonances of free UBM2 and the UBM2-ubiquitin complex were assigned by standard 3D triple-resonance experiments, and side chain resonances were assigned using 3D HCCH-TOCSY and ^{15}N- or ^{13}C-separated NOESY-HSQC experiments (Cavanagh et al., 2007). Intermolecular NOEs were initially identified by recording (1) [F1] ^{13}C-purged, [F2] ^{13}C-separated NOESY-HSQC spectra in D_2O and (2) [F1] ^{13}C-selected, [F2] ^{15}N-separated NOESY-HSQC spectra in H_2O using samples of the UBM2-ubiquitin complex with one component ^{13}C-labeled and the other component ^{15}N-labeled (Zwahlen et al., 1997). Additional intermolecular NOEs were obtained from regular ^{13}C- or ^{15}N-separated NOESY-HSQC experiments using uniformly $^{13}C/^{15}N$-labeled UBM2-ubiquitin samples. Residual dipolar couplings ($^1D_{HN}$, $^1D_{H\alpha C\alpha}$) of the free UBM2 and UBM2-ubiquitin complex were determined from the difference in couplings between an isotropic and a liquid crystalline Pf1 phage sample. A 2D ^1H-^{15}N IPAP experiment (Ottiger et al., 1998) and a modified, $J_{H\alpha C\alpha}$-coupled (HACACO)NH experiment (Ball et al., 2006) were used to measure the $^1D_{HN}$ and $^1D_{H\alpha C\alpha}$ couplings, respectively. NMR data were processed by NMRPIPE (Delaglio et al., 1995) and analyzed with XEASY/CARA (Bartels et al., 1995). NOE crosspeaks from the ^{15}N- or ^{13}C-separated NOESY-HSQC, [F1] ^{13}C-purged, [F2] ^{13}C-separated NOESY-HSQC and [F1] ^{13}C-selected, [F2] ^{15}N-separated NOESY-HSQC experiments were analyzed with a combination of manual and automated assignment and converted into distance constraints using the CALIBRATION module in CYANA (Güntert, 2004; Herrmann et al., 2002). Dihedral angles were derived from TALOS analysis of chemical shift information (Cornilescu et al., 1999) and from analysis of local NOE patterns. Initial

structures were generated with CYANA (Güntert, 2004; Herrmann et al., 2002) and then refined using XPLOR-NIH (Schwieters et al., 2003). Because the NOE-based structural ensemble of UBM2 did not display noticeable conformational changes in the ubiquitin-bound complex, both sets of RDCs of UBM2 were used for the refinement of free UBM2 and the UBM2-ubiquitin complex.

The final structural ensembles (25 structures) of the UBM2 or the UBM2-ubiquitin complex display no NOE violations > 0.5 Å and no dihedral angle violations > 5 °. The quality of these structures can be evaluated in Supplementary Tables S1 and S2.

Isothermal Titration Calorimetry

Wild-type or mutant human ubiquitin (final concentrations in the 3–6 mM range) was titrated into a solution of the human pol ι UBM2 (wild-type and mutants, 0.3–0.6 mM range) in a buffer containing 25 mM sodium phosphate, 100 mM KCl, pH 7.0. Thirty injections of 10 μl each were performed at 25 °C using a VP-ITC Microcalorimeter (GE Healthcare), and data were analyzed using the Origin software assuming one-site binding (Origin Lab).

Localization Experiments

MRC5 cells were grown on coverslips and transfected with Fugene 6 (Roche). 48–72 hours after transfection, cells were washed in PBS and fixed in 2% paraformaldehyde (PFA) for 20 minutes at room temperature. For EYFP-fused human pol ι samples, after two washes in PBS, coverslips were mounted on aqueous mounting medium (Biomeda) containing DAPI (Molecular Probes) placed on a glass holder. For FLAG-tagged constructs of mouse pol ι, after being fixed, cells were permeabilized for 10 minutes at room temperature, with a 0.2% Triton-X-100 solution in PBS. Samples were blocked overnight at 4 °C in PBS containing 5% BSA and 0.1% Tween-20. Primary and secondary antibodies were diluted in the blocking solution, and washes were performed in PBS with 0.1% Tween-20. The primary, anti-FLAG antibodies were purchased from Sigma (M2 Cat. No. F3165), and the secondary anti-mouse Cy3-conjugated antibodies were from Jackson ImmunoResearch (Cat. No. 715-165-150). Images were acquired using a ZEISS LSM 510 META laser scanning microscope. For quantification of the percentage of cells with pol ι foci formation, 1500 nuclei from three equivalent samples were scored overall for each construct. A Student's t-test was used to compare different constructs.

Yeast Strains and Plasmids

The *S. cerevisiae* strains used in this study are derivatives of W1588-4A, which are W303 strains corrected for *RAD5* (Zhao et al., 1998). The *rev1Δ* strain was constructed by moving the *rev1::kanMX4* cassette from the deletion library into W15488-4A.

DNA Damage Sensitivity and Mutagenesis Assays

For MMS and UV sensitivity assays, three independent colonies of each strain were grown in Synthetic Complete (SC) media lacking uracil (SC-Ura) and supplemented with 2% glucose at 30 °C to a density of ~2×10^7 cells/mL. Serial dilutions of the cells were plated on SC-Ura media containing 0.018% MMS. For UV sensitivity assays, appropriately diluted cells plated on SC-Ura media were irradiated at 1 J/m^2/s for 30 seconds using a G15T8 UV lamp (General Electric) at 254 nm to produce a UV dose of 30 J/m^2. Colonies were counted after growing the cells for 2 days at 30°C.

For UV reversion assays, three independent colonies of each strain were grown at 30 °C in SC-Ura media to a density of ~2×10^8 cells/mL. Appropriate dilutions of the cells were plated on SC media to monitor survival. Mutation frequencies were analyzed by plating undiluted

aliquots on SC-Ade to score for reversion of the *ade2-1* allele. Cells were exposed to a low dose of UV irradiation (1 J/m^2/s for 15 seconds using a G15T8 UV lamp at 254 nm) and grown for 3–4 or 6–7 days at 30 °C in the dark for survival or mutagenesis assays, respectively. The reversion frequencies were calculated by subtracting the spontaneous value from the frequency obtained at the 15 J/m^2 UV dose.

Supplementary Material

Refer to Web version on PubMed Central for supplementary material.

Acknowledgments

This research was supported by grants from the National Institute of General Medical Sciences GM-079376 and the Whitehead Foundation (to PZ), from the National Institute of Environmental Health Sciences ES-015818 and an American Cancer Society Research Professorship (to GCW), from the National Institute of Environmental Health Sciences P30 ES-002109 (to the Center of Environmental Health Sciences, MIT), and from the Deutsche Forschungsgemeinschaft and the Cluster of Excellence “Macromolecular Complexes” of the Goethe University Frankfurt EXC115 (to ID). MB is a recipient of the “J. Buchmann” Scholarship.

References

Akutsu M, Kawasaki M, Katoh Y, Shiba T, Yamaguchi Y, Kato R, Kato K, Nakayama K, Wakatsuki S. Structural basis for recognition of ubiquitinated cargo by Tom1-GAT domain. FEBS Lett 2005;579:5385–5391. [PubMed: 16199040]

Ball G, Meenan N, Bromek K, Smith BO, Bella J, Uhrin D. Measurement of one-bond 13Calpha-1Halpha residual dipolar coupling constants in proteins by selective manipulation of CalphaHalpha spins. J Magn Reson 2006;180:127–136. [PubMed: 16495100]

Bartels C, Xia T, Billeter M, Güntert P, Wüthrich K. The program XEASY for computer-supported NMR spectral analysis of biological macromolecules. J Biol NMR 1995;6:1–10.

Bienko M, Green CM, Crosetto N, Rudolf F, Zapart G, Coull B, Kannouche P, Wider G, Peter M, Lehmann AR, et al. Ubiquitin-binding domains in Y-family polymerases regulate translesion synthesis. Science 2005;310:1821–1824. [PubMed: 16357261]

Bomar MG, Pai MT, Tzeng SR, Li SS, Zhou P. Structure of the ubiquitin-binding zinc finger domain of human DNA Y-polymerase eta. EMBO Rep 2007;8:247–251. [PubMed: 17304240]

Cavanagh, J.; Fairbrother, WJ.; Palmer, AGr; Skelton, NJ.; Rance, M. Protein NMR Spectroscopy: Principles and Practice. Burlington, MA: Elsevier Academic Press; 2007.

Chang YG, Song AX, Gao YG, Shi YH, Lin XJ, Cao XT, Lin DH, Hu HY. Solution structure of the ubiquitin-associated domain of human BMSC-UbP and its complex with ubiquitin. Protein Sci 2006;15:1248–1259. [PubMed: 16731964]

Chen ZJ, Sun LJ. Nonproteolytic functions of ubiquitin in cell signaling. Molecular cell 2009;33:275–286. [PubMed: 19217402]

Clore GM, Garrett DS. R-factor, Free R, and complete cross-validation for dipolar coupling refinement of NMR structures. J Am Chem Soc 1999;121:9008–9012.

Cornilescu G, Delaglio F, Bax A. Protein backbone angle restraints from searching a database for chemical shift and sequence homology. J Biomol NMR 1999;13:289–302. [PubMed: 10212987]

D’Souza S, Waters LS, Walker GC. Novel conserved motifs in Rev1 C-terminus are required for mutagenic DNA damage tolerance. DNA repair 2008;7:1455–1470. [PubMed: 18603483]

Davis IW, Murray LW, Richardson JS, Richardson DC. MOLPROBITY: structure validation and all-atom contact analysis for nucleic acids and their complexes. Nucleic Acids Res 2004;32:W615–W619. [PubMed: 15215462]

Delaglio F, Grzesiek S, Vuister GW, Zhu G, Pfeifer J, Bax A. NMRPipe: a multidimensional spectral processing system based on UNIX pipes. J Biomol NMR 1995;6:277–293. [PubMed: 8520220]

Dumstorf CA, Mukhopadhyay S, Krishnan E, Haribabu B, McGregor WG. REV1 is implicated in the development of carcinogen-induced lung cancer. Mol Cancer Res 2009;7:247–254. [PubMed: 19176310]

Gueranger Q, Stary A, Aoufouchi S, Faili A, Sarasin A, Reynaud CA, Weill JC. Role of DNA polymerases eta, iota and zeta in UV resistance and UV-induced mutagenesis in a human cell line. DNA repair 2008;7:1551–1562. [PubMed: 18586118]

Güntert P. Automated NMR structure calculation with CYANA. Methods Mol Biol 2004;278:353–378. [PubMed: 15318003]

Guo C, Sonoda E, Tang TS, Parker JL, Bielen AB, Takeda S, Ulrich HD, Friedberg EC. REV1 protein interacts with PCNA: significance of the REV1 BRCT domain in vitro and in vivo. Molecular cell 2006a;23:265–271. [PubMed: 16857592]

Guo C, Tang TS, Bienko M, Dikic I, Friedberg EC. Requirements for the interaction of mouse Polkappa with ubiquitin and its biological significance. The Journal of biological chemistry 2008;283:4658–4664. [PubMed: 18162470]

Guo C, Tang TS, Bienko M, Parker JL, Bielen AB, Sonoda E, Takeda S, Ulrich HD, Dikic I, Friedberg EC. Ubiquitin-binding motifs in REV1 protein are required for its role in the tolerance of DNA damage. Mol Cell Biol 2006b;26:8892–8900. [PubMed: 16982685]

Herrmann T, Güntert P, Wüthrich K. Protein NMR structure determination with automated NOE assignment using the new software CANDID and the torsion angle dynamics algorithm DYANA. J Mol Biol 2002;319:209–227. [PubMed: 12051947]

Hirano S, Kawasaki M, Ura H, Kato R, Raiborg C, Stenmark H, Wakatsuki S. Double-sided ubiquitin binding of Hrs-UIM in endosomal protein sorting. Nat Struct Mol Biol 2006;13:272–277. [PubMed: 16462748]

Hoege C, Pfander B, Moldovan GL, Pyrowolakis G, Jentsch S. RAD6-dependent DNA repair is linked to modification of PCNA by ubiquitin and SUMO. Nature 2002;419:135–141. [PubMed: 12226657]

Hofmann K. Ubiquitin-binding domains and their role in the DNA damage response. DNA repair 2009;8:544–556. [PubMed: 19213613]

Kang RS, Daniels CM, Francis SA, Shih SC, Salerno WJ, Hicke L, Radhakrishnan I. Solution structure of a CUE-ubiquitin complex reveals a conserved mode of ubiquitin binding. Cell 2003;113:621–630. [PubMed: 12787503]

Kannouche PL, Wing J, Lehmann AR. Interaction of human DNA polymerase eta with monoubiquitinated PCNA: a possible mechanism for the polymerase switch in response to DNA damage. Molecular cell 2004;14:491–500. [PubMed: 15149598]

Lee S, Tsai YC, Mattera R, Smith WJ, Kostelansky MS, Weissman AM, Bonifacino JS, Hurley JH. Structural basis for ubiquitin recognition and autoubiquitination by Rabex-5. Nat Struct Mol Biol 2006;13:264–271. [PubMed: 16462746]

Lin X, Okuda T, Trang J, Howell SB. Human REV1 modulates the cytotoxicity and mutagenicity of cisplatin in human ovarian carcinoma cells. Molecular pharmacology 2006;69:1748–1754. [PubMed: 16495473]

Liu G, Warbrick E. The p66 and p12 subunits of DNA polymerase delta are modified by ubiquitin and ubiquitin-like proteins. Biochemical and biophysical research communications 2006;349:360–366. [PubMed: 16934752]

Mirchandani KD, McCaffrey RM, D'Andrea AD. The Fanconi anemia core complex is required for efficient point mutagenesis and Rev1 foci assembly. DNA repair 2008;7:902–911. [PubMed: 18448394]

Niedzwiedz W, Mosedale G, Johnson M, Ong CY, Pace P, Patel KJ. The Fanconi anaemia gene FANCC promotes homologous recombination and error-prone DNA repair. Molecular cell 2004;15:607–620. [PubMed: 15327776]

Ohmori H, Friedberg EC, Fuchs RP, Goodman MF, Hanaoka F, Hinkle D, Kunkel TA, Lawrence CW, Livneh Z, Nohmi T, et al. The Y-family of DNA polymerases. Molecular cell 2001;8:7–8. [PubMed: 11515498]

Ohno A, Jee J, Fujiwara K, Tenno T, Goda N, Tochio H, Kobayashi H, Hiroaki H, Shirakawa M. Structure of the UBA domain of Dsk2p in complex with ubiquitin molecular determinants for ubiquitin recognition. Structure 2005;13:521–532. [PubMed: 15837191]

Okuda T, Lin X, Trang J, Howell SB. Suppression of hREV1 expression reduces the rate at which human ovarian carcinoma cells acquire resistance to cisplatin. Molecular pharmacology 2005;67:1852–1860. [PubMed: 15758147]

Ottiger M, Delaglio F, Bax A. Measurement of J and dipolar couplings from simplified two-dimensional NMR spectra. J Magn Reson 1998;131:373–378. [PubMed: 9571116]

Penengo L, Mapelli M, Murachelli AG, Confalonieri S, Magri L, Musacchio A, Di Fiore PP, Polo S, Schneider TR. Crystal structure of the ubiquitin binding domains of rabex-5 reveals two modes of interaction with ubiquitin. Cell 2006;124:1183–1195. [PubMed: 16499958]

Plosky BS, Vidal AE, Fernandez de Henestrosa AR, McLenigan MP, McDonald JP, Mead S, Woodgate R. Controlling the subcellular localization of DNA polymerases iota and eta via interactions with ubiquitin. Embo J 2006;25:2847–2855. [PubMed: 16763556]

Prag G, Lee S, Mattera R, Arighi CN, Beach BM, Bonifacino JS, Hurley JH. Structural mechanism for ubiquitinated-cargo recognition by the Golgi-localized, gamma-ear-containing, ADP-ribosylation-factor-binding proteins. Proc Natl Acad Sci U S A 2005;102:2334–2339. [PubMed: 15701688]

Richardson JS, Richardson DC. Amino acid preferences for specific locations at the ends of alpha helices. Science 1988;240:1648–1652. [PubMed: 3381086]

Sabbioneda S, Gourdin AM, Green CM, Zotter A, Giglia-Mari G, Houtsmuller A, Vermeulen W, Lehmann AR. Effect of proliferating cell nuclear antigen ubiquitination and chromatin structure on the dynamic properties of the Y-family DNA polymerases. Mol Biol Cell 2008;19:5193–5202. [PubMed: 18799611]

Schwieters CD, Kuszewski JJ, Tjandra N, Clore GM. The Xplor-NIH NMR molecular structure determination package. J Magn Reson 2003;160:65–73. [PubMed: 12565051]

Swanson KA, Hicke L, Radhakrishnan I. Structural basis for monoubiquitin recognition by the Ede1 UBA domain. J Mol Biol 2006;358:713–724. [PubMed: 16563434]

Swanson KA, Kang RS, Stamenova SD, Hicke L, Radhakrishnan I. Solution structure of Vps27 UIM-ubiquitin complex important for endosomal sorting and receptor downregulation. Embo J 2003;22:4597–4606. [PubMed: 12970172]

Wang Q, Young P, Walters KJ. Structure of S5a bound to monoubiquitin provides a model for polyubiquitin recognition. J Mol Biol 2005;348:727–739. [PubMed: 15826667]

Watanabe K, Tateishi S, Kawasuji M, Tsurimoto T, Inoue H, Yamaizumi M. Rad18 guides poleta to replication stalling sites through physical interaction and PCNA monoubiquitination. Embo J 2004;23:3886–3896. [PubMed: 15359278]

Wood A, Garg P, Burgers PM. A ubiquitin-binding motif in the translesion DNA polymerase Rev1 mediates its essential functional interaction with ubiquitinated proliferating cell nuclear antigen in response to DNA damage. The Journal of biological chemistry 2007;282:20256–20263. [PubMed: 17517887]

Zhao X, Muller EG, Rothstein R. A suppressor of two essential checkpoint genes identifies a novel protein that negatively affects dNTP pools. Molecular cell 1998;2:329–340. [PubMed: 9774971]

Zhou P, Lugovskoy AA, Wagner G. A solubility-enhancement tag (SET) for NMR studies of poorly behaving proteins. J Biomol NMR 2001;20:11–14. [PubMed: 11430750]

Zwahlen C, Legault P, Vincent SJF, Greenblatt J, Konrat R, Kay LE. Methods for Measurement of Intermolecular NOEs by Multinuclear NMR Spectroscopy: Application to a Bacteriophage N-Peptide/boxB RNA Complex. J Am Chem Soc 1997;119:6711–6721.

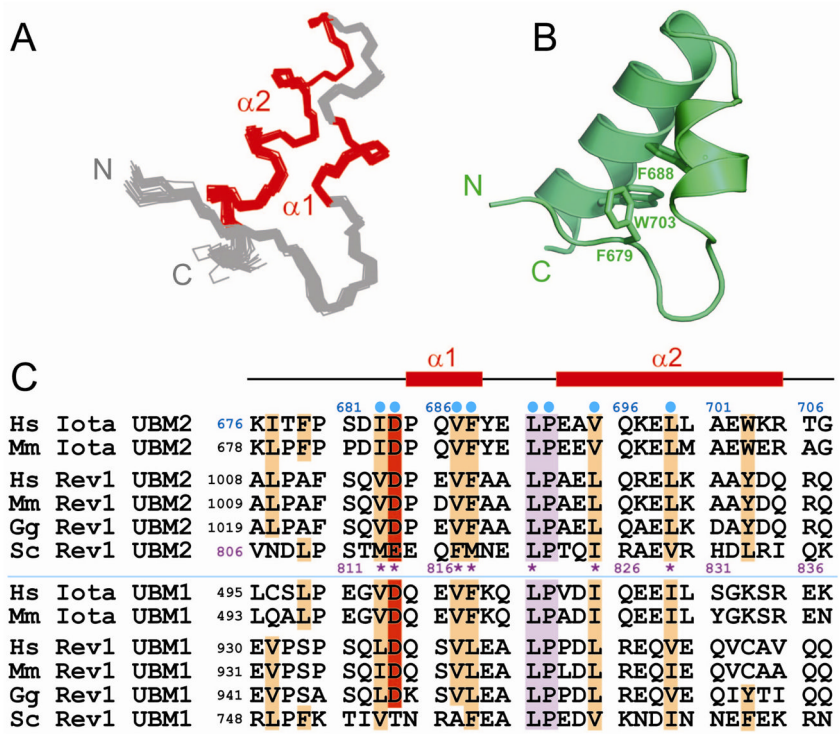

Figure 1.

Structure of the human pol ι UBM2. (A) Backbone traces of the NMR ensemble of 25 structures. Helices and loops are colored in red and grey, respectively. (B) Ribbon diagram. Core aromatic residues are shown in the stick model. (C) Sequence alignment of UBMs. Conserved residues are highlighted, with the signature “Leu-Pro” motif in purple, hydrophobic residues in brown and negatively charged residues in red. Pol ι UBM2 mutations evaluated for ubiquitin binding and foci formation are labeled with blue circles, and Rev1 UBM2 mutants assayed for DNA damage response are indicated by purple asterisks. The listed genes are *Homo sapiens* (Hs) pol ι: AF245438; *Mus musculus* (Mm) pol ι: AAS75834; Hs Rev1 AAI30412; Mm Rev1 AAF23323; *Gallus gallus* (Gg) Rev1 AAV80844; *Saccharomyces cerevisiae* (Sc) Rev1: NP_014991.

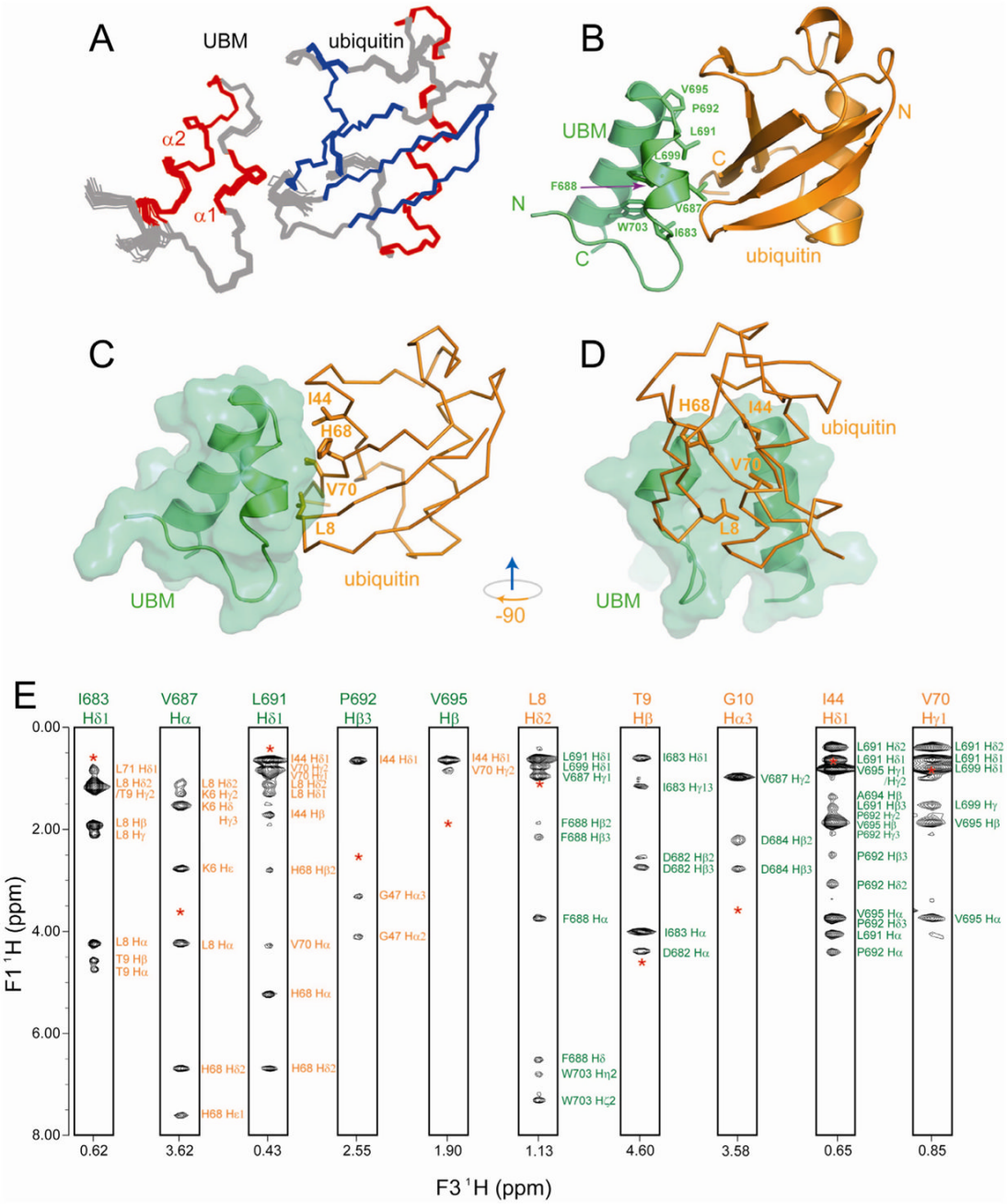

Figure 2.

Structure of the human pol ι UBM2-ubiquitin complex. (A) Backbone traces of the NMR ensemble of 25 structures. Strands, helices and loops are colored in blue, red, and grey, respectively. (B) Ribbon diagram of the complex, with UBM2 in pale green and ubiquitin in orange. Side chains of ubiquitin-interacting residues are shown in the stick model. Side view (C) and front view (D) of the ubiquitin-binding interface on UBM2 depict an interaction network centered at L8, instead of I44, of ubiquitin. (E) Representative strips of intermolecular NOE crosspeaks between UBM2 and ubiquitin from the [F1] ^{13}C-purged, [F2] ^{13}C-separated NOESY-HSQC spectra. Only one of the two binding partners is ^{13}C-labeled. Red asterisks

indicate proton diagonal positions. Resonances of UBM2 and ubiquitin are colored in pale green and orange, respectively.

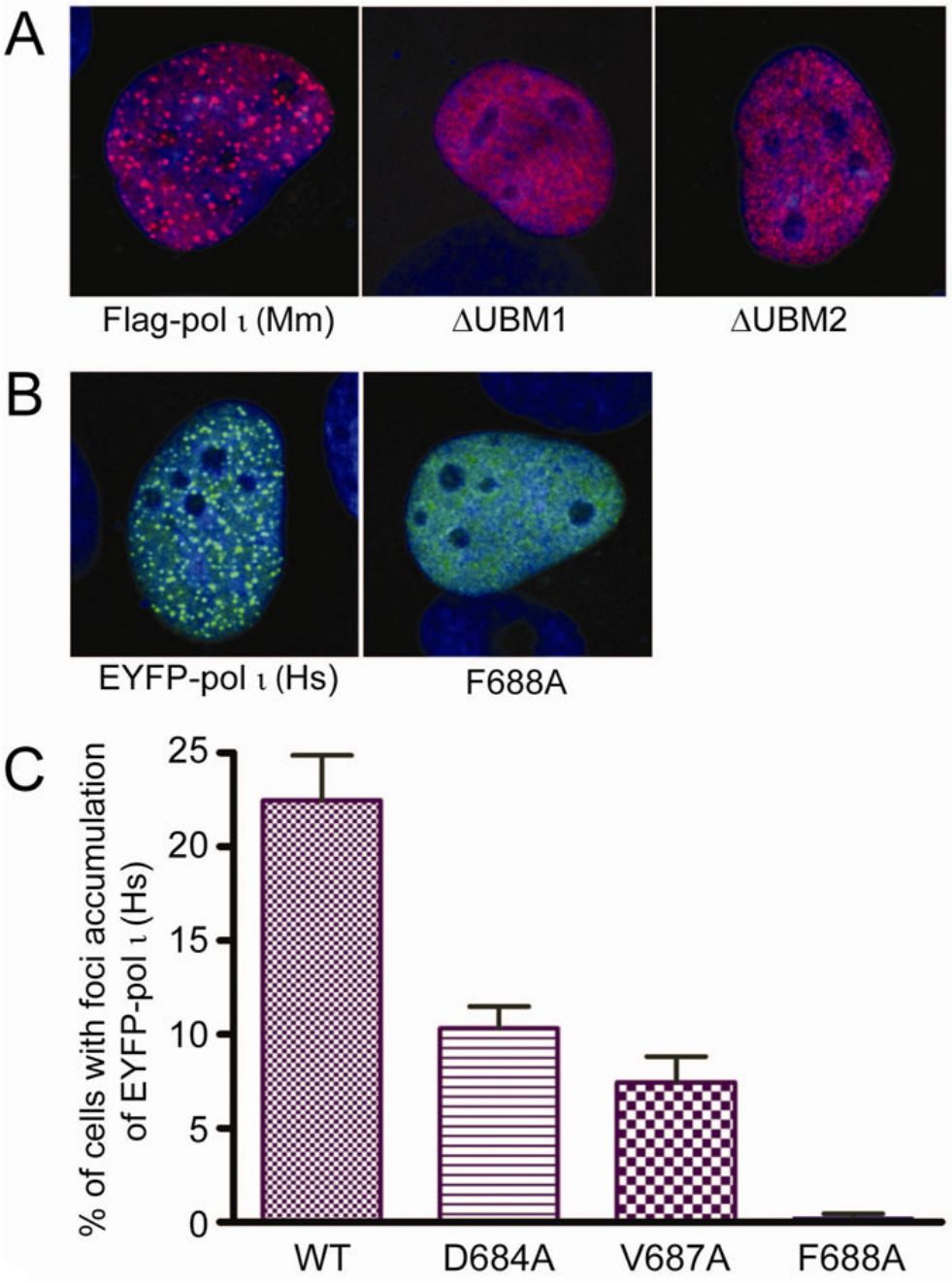

Figure 3.

UBM-ubiquitin binding is required for pol ι to accumulate in replication foci. (A) Representative foci formation in MRC5 cells transfected with mouse FLAG-tagged WT (left), ΔUBM1 (middle) or ΔUBM2 (right) pol ι. (B) Representative foci formation in MRC5 cells transfected with human EYFP-fused WT (left) or F688A (right) pol ι. (C) Percentages of MRC5 cells with foci accumulation of human EYFP-pol ι UBM2 mutants. Error bars indicate the standard deviation of three independent measurements.

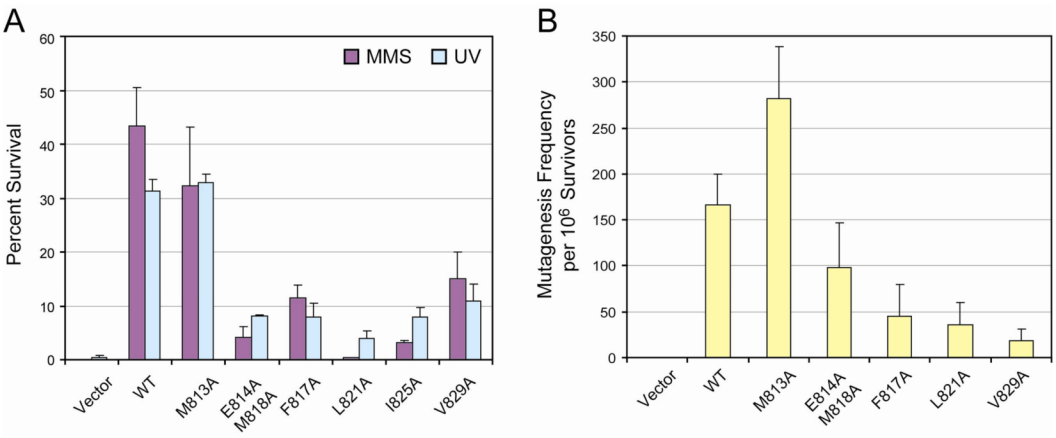

Figure 4.

Mutations of ubiquitin-binding residues in *S. cerevisiae* Rev1 UBM2 impair *REV1*-mediated survival and mutagenesis. (A) Survival of Rev1 UBM2 point mutants after MMS treatment (0.018%) or UV irradiation (30 J/m^2). (B) Reversion frequency for Rev1 UBM2 mutants after a dose of UV irradiation (15 J/m^2). Error bars represent the standard deviation of three independent measurements.

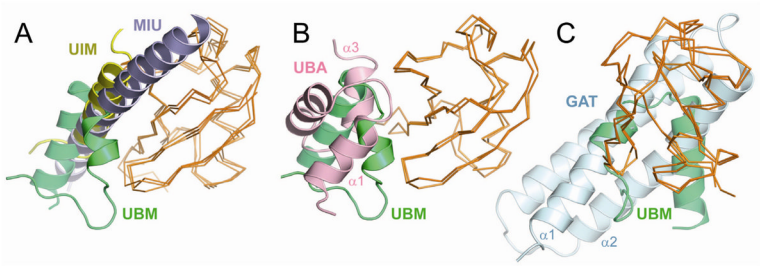

Figure 5.

A distinct mode of ubiquitin recognition by UBM. (A) Ubiquitin binding by UIM (yellow, PDB 1Q0W) and IUIM/MIU (light blue, PDB 2FID) occurs via a single helix. Ubiquitin binding by three-helix bundle domains UBA (pink, PDB 2G3Q) and GAT (light cyan, PDB 1YD8) is shown in panels (B) and (C) respectively. UBM is colored in pale green. Ubiquitin orientations are identical to that in Figure 2C or 2D.

Table 1

Binding Constants Measured by ITC

UBM2	Ubiquitin	K_d
WT	WT	15 μM
I683A	WT	78 μM
D684A	WT	NDB
D684T	WT	NDB
V687A	WT	94 μM
F688A	WT	NDB
L691A	WT	110 μM
P692A	WT	167 μM
L691A/P692A	WT	NDB
V695A	WT	295 μM
L699A	WT	186 μM
WT	L8A	NDB
WT	I44A	83 μM
WT	H68A	62 μM
WT	V70A	167 μM

NDB: No detectable binding or too weak to fit reliably (K_d > 400 μM)